Rotational-translational relaxation effects in diatomic-gas flows

V.V. Riabov

Department of Computer Science, Rivier College, Nashua, New Hampshire 03060 USA

1 Introduction

The problem of deriving the nonequilibrium gas dynamic equations from the first principles of the kinetic theory of gases was studied by Ferziger and Kaper [1] in the cases of near-equilibrium and slow-relaxation processes of the energy exchange between internal and translational degrees of molecular freedom. The case of the arbitrary energy exchange ratio was analyzed in [2], [3], [4], [5] for polyatomic gas mixtures.

In the present study the problem of redistribution of translational and rotational energy has been solved for diatomic gases within the framework of the Chapman-Enskog method [1], [5], [6] and the Parker model [7] in the general case of the arbitrary energy exchange ratio. The gasdynamic equations, transport coefficients and relaxation time have been found for nonequilibrium processes in diatomic gases [5], [6]. The calculations of relaxation time, viscosity, thermal conductivity, and diffusion coefficients are carried out in the temperature range from 200 K to 10,000 K for nitrogen by using the technique of integral brackets [1], [4]. The calculated parameters are compared with the values obtained by the approximate method [8] as well as data from experiments [9], [10] in ultrasonic, shock-wave, and vacuum devices. The correlation of theoretical and experimental data is satisfactory. The applicability of one- and two-temperature relaxation models for para-hydrogen at the rotational temperature range from 0 to 1200 K is discussed. The numerical solutions of the Navier-Stokes equations are analyzed for spherical expanding nitrogen flow and supersonic flow near a sphere.

2 Rotational relaxation time estimations

Two definitions of relaxation time are widely used. In the first case the expression for the temperature dependence of the relaxation time, $\tau_{\mathrm{R1}}(T)$, is obtained by using the Chapman-Enskog iteration method of solving the Boltzmann equation for a gas of particles with internal degrees of freedom [1]. In the second case the relaxation time, $\tau_{\mathrm{R2}}(T)$, is found directly from the relaxation equation (see Eq. (17) from [6]) by calculating the rate of increase of the internal energy of the molecules that originally were not excited [11].

In the present study parameters $p\tau_{\mathrm{R1}}(T)$ and $p\tau_{\mathrm{R2}}(T)$ are calculated for nitrogen by formulas (18)-(20) from [6]. Multifold integrals are calculated at 200 points over the range 200 K $\leq T \leq$ 10,000 K, using the Monte-Carlo technique [5], with 4000 tests at each point. The data for intermediate points are determined by using cubic splines [6]. The estimated accuracy of the calculations is 1.5 percent. The higher orders of the theory of perturbations [6] make a substantial contribution at $T <$ 400 K, and the accuracy of the calculations is lower under these conditions. The results of calculations $p\tau_{\mathrm{R2}}$ and $p\tau_{\mathrm{R1}}$

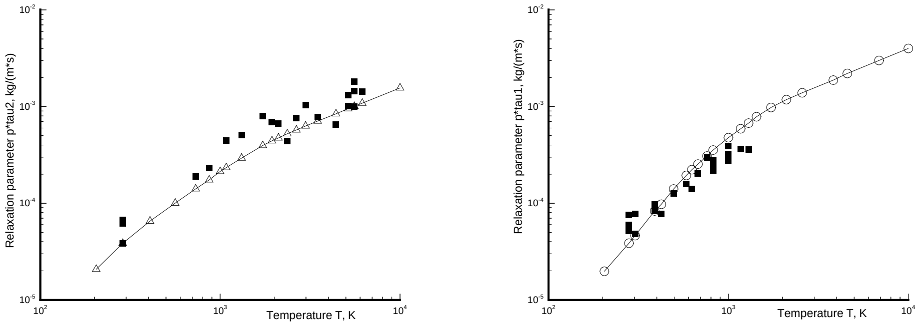

Fig. 1. Parameters $p\tau_{\mathrm{R}2}$ (*left*) and $p\tau_{\mathrm{R}1}$ (*right*) versus temperature T

are shown in Fig. 1 (solid lines). The experimental data (filled squares) were acquired in [9], [10]. The calculations show that at 200 K $\leq T \leq$ 10,000 K, $p\tau_{\mathrm{R}1}$ is 2 or 2.5 times as large as $p\tau_{\mathrm{R}2}$. This difference is apparently due to the adiabatic nature of the energy exchange between the highly excited rotational states of the molecules [5]. The effect of the initial energy distribution at rotational levels was not considered in this comparison. The quantity $p\tau_{\mathrm{R}1}(T)$ was used for interpreting the experimental data on the scattering and absorption of ultrasound, where the effect of the ultrasound frequency on $p\tau_{\mathrm{R}1}$ was disregarded [9]. The quantity $p\tau_{\mathrm{R}2}(T)$ was used for interpreting the data of experiments in shock tubes. The available experimental data [9], [10], both on ultrasound and on shock waves, differ from one another by 200-300 percent, which is approximately equal to the difference between $p\tau_{\mathrm{R}1}$ and $p\tau_{\mathrm{R}2}$, as evident from Fig. 1.

3 The effect of initial rotational energy distribution

The effect of the initial energy distribution at rotational levels has been estimated in [5] under the assumption that at initial time the distribution corresponds to the Boltzmann distribution with rotational temperature $T_{\mathrm{R}} > 0$. Therefore, the translational-rotational relaxation time becomes a function of both T and T_{R} (see Eq. (1.7) in [5]). The parameter $p\tau_{\mathrm{R}2}(T, T_{\mathrm{R}})$, calculated for nitrogen at $T = 1000$ K, decreases from 2.13×10^{-4} kg/(m·s) for $T_{\mathrm{R}} = 0$ K to 5.24×10^{-5} kg/(m·s) for $T_{\mathrm{R}} = 800$ K.

The problem of a proper selection of the relaxation time $[\tau_{\mathrm{R}2}(T)$ versus $\tau_{\mathrm{R}2}(T, T_{\mathrm{R}})]$ for a more accurate description of the manner in which the system approaches equilibrium is studied for para-hydrogen. The solution of the kinetic equation in τ approximation (see Eq. (17) in [6]) was compared with the solution obtained by numerical integration of the system of kinetic equations for the occupancies of the individual rotational levels [5]. In these calculations, the constants of the rotational-transfer rates were estimated within the framework of the effective-potential method [12]. The calculation results are shown in Fig. 2 (*left*), where parameters $p\tau_{\mathrm{R}2}(T, T_{\mathrm{R}})$, estimated at constant temperature $T =$ 400 K, (triangles) are compared with the results of numerical integration of the system of kinetic equations (circles). The point $T_{\mathrm{R}} = 0$ K of the first curve corresponds to $p\tau_{\mathrm{R}2}(T)$. A dependence of the relaxation time on T_{R} is observed. Therefore, the use of a function

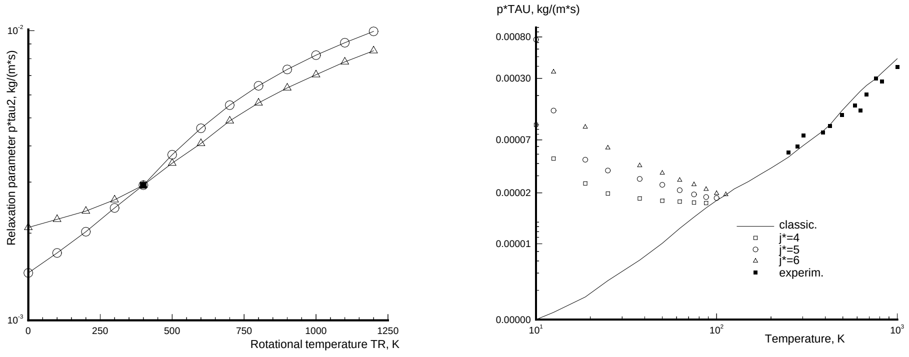

Fig. 2. The rotational relaxation parameters $p\tau_{R2}(T,\, T_R)$ in para-hydrogen at constant temperature $T = 400$K (*left*) and in nitrogen expanding into a vacuum (*right*)

$p\tau_{R2}(T,\, T_R)$ significantly improves the approximate solution of the relaxation equation, and the initial distribution of energy at rotational levels should be taken into account within the framework of the τ approximation.

4 Rotational relaxation in freely expanding gas flows

Studies [13], [14] of the rotational relaxation in expanding gas flows discovered a significant decrease of the gas density downstream that leads to a decrease in the number of molecular collisions. The departure of the gas rotational energy from the equilibrium value was observed.

Lebed and Riabov [15], [16] studied another cause for the rotational energy departure. At the decrease of kinetic temperature T_t, adiabatic collision conditions [17] should be taken into account, and the relaxation time τ_R increases due to the sharp decrease of the rotational transfer probabilities. Using this method [15], the relaxation times were calculated for nitrogen at stagnation temperature $T_0 = 295$ K [see Fig. 2 (*right*)] under the conditions of aerodynamic experiments in underexpanded jets [13], [14], [16]. The calculations based on the classical concept [7] [see solid line in Fig. 2 (*right*)] do not show a tendency of increasing $p\tau_R$ with the decrease of T_t under adiabatic rotational energy exchange conditions. At temperatures $T_t > 273$ K, numerical results correlate well with experimental data [9], [10]. In the expansion of nitrogen, starting at $T_0 =$ 300 K, the maximum population of molecules occurs at rotational levels J from 6 to 4 [15], [17]. The results of calculating $p\tau_R$ for $J = 6$, 5, and 4 are shown in Fig. 2 (*right*) (empty triangles, circles, and squares, correspondingly). The values of $p\tau_R$ increase with decrease of T_t. At $T_t > 100$ K, the adiabatic condition breaks down, and the parameter $p\tau_R$ could be estimated by the Parker's model [7].

For qualitative estimations, the energy relaxation time is replaced by the relaxation time of the level J. This approximate method [15] correctly represents the nature of the R-T nonequilibrium process, i.e., an increase of $p\tau_R$ with decreasing T_t. Figure 3 (*left*) shows the distributions of rotational temperature T_R along the axis of nitrogen jet. The result of using the classical mechanics concept [7] is shown there by diamonds. The curves

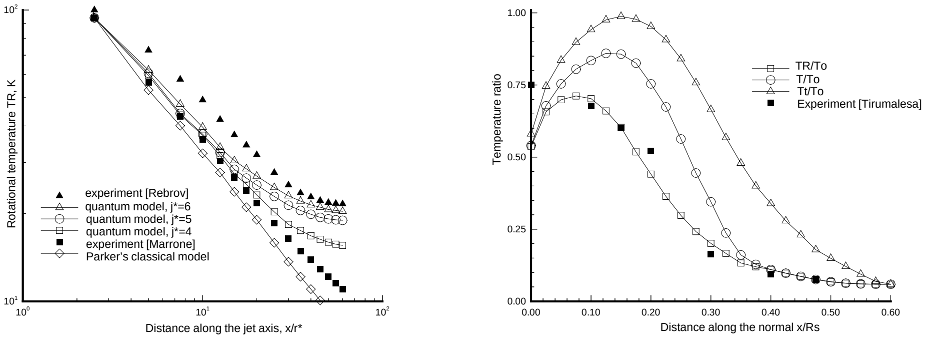

Fig. 3. The rotational T_{R} and translational T_{t} temperatures in spherically expanding flow of nitrogen (*left*) and at the stagnation streamline near a sphere (*right*)

marked by empty triangles, circles, and squares were obtained for values of $p\tau_{\mathrm{R}}$ at $J =$ 6, 5, and 4, correspondingly. The calculations were made at K $= \rho ur/(p\tau_{\mathrm{R}}) = 2730$, $p_0 r_{\mathrm{j}}$ $= 240$ torr·mm and $T_0 = 295$ K.

The experimental data ((filled squares) [13], (triangles) [14]) for T_{R} are upper and lower bounds on the distribution of rotational energy along the nitrogen jet. Numerical results, based on the quantum concept of rotational energy exchange, correlate well with the experimental data [14]. The data contradicts the classical model predictions [7] of T_{R}. The experimental and computational results demonstrate the necessity of considering the quantum concept in describing R-T relaxation in underexpanded jets. This concept was used in evaluating various relaxation models in expanding low-density nitrogen flows [18].

5 Transport coefficients in non-equilibrium diatomic gases

The analytic formulas for transport coefficients were found by Lebed and Riabov (see Eqs. (21-29) in [6]): the coefficients of shear viscosity corresponding to rotationally inelastic and elastic collisions, η and η_0; the corresponding values of the thermal conductivity, λ and λ_0; and the self-diffusion coefficient of the elastically colliding molecules, D_0. The simplest approximations for the thermal conductivity coefficient λ were analyzed in [1], [5], [6], [8]. The first approximation [8] was based on the diffusive transfer, but it disregarded the relaxation of the rotational energy. The relaxation was taken into account partially in the next, second, approximation [8] for the thermal conductivity coefficient λ_2. Triangles and circles in Fig. 4 (*left*) show η and η_0, correspondingly, as given by Eqs. (21-29) from [6], while the filled squares indicate the experimental data of Vargaftik [19]. The difference between η and η_0 is evaluated as 5 percent in the low-temperature regime. At temperature $T > 1000$ K these values correlate well with each other. The parameter $\rho D_0/\eta_0$ is approximately constant and equals to 1.20.

Triangles in Fig. 4 (*right*) show λ, as given by Eqs. (21-29) from [6]. Circles correspond to the Mason and Monchick's second approximation [8], λ_2. The filled squares indicate the experimental data of Vargaftik [19]. The present analysis shows that the correlation between the exact solution, the Mason and Monchick's second approximation [8], and

Home

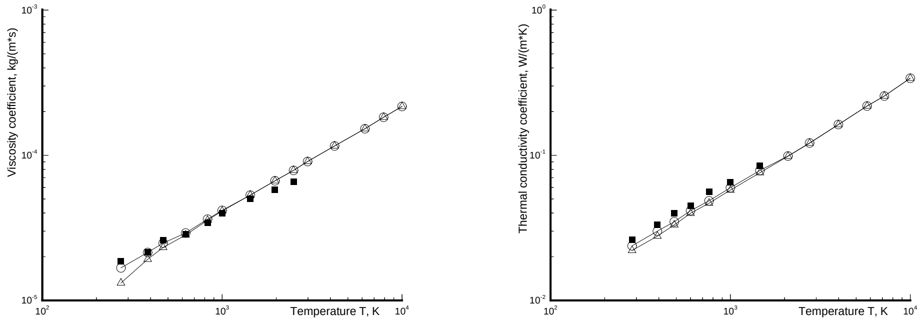

Fig. 4. Viscosity (*left*) and conductivity coefficients (*right*) in nitrogen

experimental data [19] is acceptable. The small discrepancy between the theoretical values of η and λ and the experimental data (see Fig. 4) can be eliminated by a proper choice of the molecule collision potential at $T < 1000$ K.

6 Rotational relaxation in viscous gas flow near a sphere

The combined effect of the rotational-translational relaxation and the viscosity and thermal conductivity processes is studied here by solving the full system of the Navier-Stokes equations and the relaxation equation (see Eq. (42-46) from [6]) with the implicit numerical technique [20]. The flow of molecular nitrogen was assumed to be undisturbed on the outer boundary of the computational region. At the spherical surface the slip, temperature and rotational energy jump conditions [20] were used.

The distributions of the nonequilibrium rotational (T_R, empty squares) and translational (T_t, triangles) temperatures are shown in Fig. 3 (*right*) for flow at Knudsen number $Kn = 0.08$ (or Reynolds number $Re_0 = 16.86$), Mach number $M = 9$, stagnation temperature $T_0 = 298$ K, and temperature factor $t_\mathrm{w} = 0.3$. In the viscous shock layer near a sphere, a significant difference between the translational and rotational temperatures can be observed. The shock-layer becomes thicker under the nonequilibrium flow conditions than in the case of equilibrium flow at $T_\mathrm{R} = T_\mathrm{t}$ [see circles in Fig. 3 (*right*)]. The numerical results for T_R correlate well with the experimental data [21] [marked by filled squares in Fig. 3 (*right*)], obtained in a wind tunnel by the electron-beam diagnostics.

7 Conclusion

The calculations of relaxation time, viscosity and thermal conductivity, and diffusion coefficients were carried out by using the Monte-Carlo simulation technique for nitrogen at 200 K $\leq T \leq$ 10,000 K . The calculations and available experimental data show that the rotational relaxation time, $\tau_{\mathrm{R}1}$, obtained by using the Chapman-Enskog iteration method, is 2 or 2.5 times as large as the time $\tau_{\mathrm{R}2}$, which is found directly from the relaxation equation. The difference is apparently due to the adiabatic nature of the energy exchange

Home

between the highly excited rotational states of the molecules. The quantity $p\tau_{\mathrm{R1}}$ is used for interpreting the experimental data on the scattering and absorption of ultrasound. The quantity $p\tau_{\mathrm{R2}}$ is used for interpreting the data of experiments in shock tubes. The use of a function $p\tau_{\mathrm{R2}}(T,\ T_{\mathrm{R}})$ significantly improves the approximate solution of the relaxation equation, and the initial distribution of energy at rotational levels should be taken into account within the framework of the τ approximation.

Acknowledgement. The author expresses gratitude to I. V. Lebed for his participation in this study.

References

1. J. Ferziger, H.G. Kaper: *Mathematical Theory of Transport Processes in Gases* (North-Holland, Amsterdam-London 1972)
2. M.N. Kogan, N.K. Makashev: Fluid Dynam. **13**, 126 (1978)
3. B.V. Alekseev: Tekhn. Eksper. Khimiya **5**, 88 (1969)
4. V.A. Matsuk, V.A. Rykov: J. Appl. Mech. Techn. Phys. **18**, 61 (1978)
5. I.V. Lebed, V.V. Riabov: J. Appl. Mech. Techn. Phys. **24**, 447 (1983)
6. V.V. Riabov: J. Thermophys. Heat Transf. **14**, 404 (2000)
7. J.G. Parker: Phys. Fluids **2**, 449 (1959)
8. E.A. Mason, L. Monchick: J. Chem. Phys. **36**, 1622 (1962)
9. C.A. Brau, R.H. Jonkman: J. Chem. Phys. **52**, 474 (1970)
10. J.A. Lordi, R.E. Mates: Phys. Fluids **13**, 291 (1970)
11. B.F. Gordiets, A.I Osipov, L.A. Shelepin: *Kinetic Processes in Gases and Molecular Lasers* (Nauka, Moscow 1980)
12. H. Rabitz, S.H. Lam: J. Chem. Phys. **63**, 3532 (1975)
13. P.V. Marrone: Phys. Fluids **10**, 521 (1967)
14. B. Borzenko, N. Karelov, A. Rebrov, R. Sharafutdinov: J. Appl. Mech. Techn. Phys. **17**, 20 (1976)
15. I.V. Lebed, V.V. Riabov: J. Appl. Mech. Techn. Phys. **20**, 1 (1979)
16. V.V. Riabov: J. Aircraft **32**, 471 (1995)
17. I.V. Lebed, S.Ya. Umanskii: Khimiya Vysokikh Energii **10**, 501 (1976)
18. L. Gochberg, B. Haas: AIAA Paper 95-2070 (1995)
19. I.B. Vargaftik: *Handbook of the Thermophysical Properties of Gases and Liquids* (Nauka, Moscow 1972)
20. V.V. Riabov: Fluid Dynam. **15**, 320 (1980)
21. D. Tirumalesa: AIAA J. **6**, 369 (1968)